Journal of Pharmaceutical and Biomedical Analysis 56 (2011) 1046–1056

Contents lists available at ScienceDirect

Journal of Pharmaceutical and Biomedical Analysis

journal homepage: www.elsevier.com/locate/jpba

Identification of the absorbed components and metabolites in rat plasma after oral administration of *Rhizoma Chuanxiong* decoction by HPLC–ESI-MS/MS

Aihua Zuo[a], Li Wang[a], Hongbin Xiao[a,*], Limin Li[b], Yuhong Liu[b], Jinhai Yi[b]

[a] Key Laboratory of Separation Science for Analytical Chemistry, Dalian Institute of Chemical Physics, Chinese Academy of Science, 457 Zhongshan Road, Dalian 116023, China
[b] Sichuan Academy of Chinese Medicine Sciences, Sichuan 610041, China

ARTICLE INFO

Article history:
Received 18 February 2011
Received in revised form 31 July 2011
Accepted 3 August 2011
Available online 10 August 2011

Keywords:
Absorbed components
HPLC–ESI-MS
Rat plasma
Ligusticum chuanxiong
Metabolism

ABSTRACT

An HPLC–ESI-MS/MS method was established to identify the absorbed components and metabolites in rat plasma after oral administration of *Rhizoma Chuanxiong* decoction (RCD), a well-known traditional Chinese medicine. By comparing the extracted ion chromatograms (EICs) obtained from dosed rat plasma, blank rat plasma and RCD, a total of 25 compounds were detected in dosed rat plasma. Among them, 13 compounds were absorbed into rat plasma in prototype and identified as ferulic acid, senkyunolide J, senkyunolide I, senkyunolide D or 4,7-dihydroxy-3-butylphthalide, senkyunolide F, senkyunolide M, senkyunolide Q, senkyunolide A, E-butylidenephthalide, E-ligustilide, neocnidilide, Z-ligustilide, levistolide A, according to the retention times, UV, MS, MS/MS spectra. In addition, 12 conjugated metabolites including 6 senkyunolide I-related metabolites, 4 senkyunolide J-related metabolites and 2 butylidenephthalide-related metabolites were also detected and identified by comparing their MS, MS/MS spectra with that of corresponding original components. Conjugated with glutathione, cysteine, glucuronic acid and sulphuric acid were the main metabolic reactions of phthalides. Finally the *in vivo* metabolic pathways of chemical constituents of Chuanxiong in rat plasma were proposed in this study.

1. Introduction

Traditional Chinese medicines (TCMs) play an important role in the clinical treatment of disease in China for centuries. However, their specific active constituents and corresponding action mechanism are still under investigation. The traditional approach to screen their active constituents generally isolate single component and *in vitro* test its bioactivity one by one. However, the overall efficacy of TCM was simply unequal to the sum of all active constituents' effects. To establish an integrated method for screening and analyzing the effective components in TCM, serum pharmacochemistry was proposed [1], which based on the hypothesis that active constituents were the components absorbed into blood. With the help of this method, the effective components of Erxian Decoction [2], She-Xiang-Bao-Xin pill [3], Dang-Gui-Bu-Xue decoction [4] were investigated by *in vivo* bioactive components fingerprint chromatogram.

Rhizoma Chuanxiong, the dried rhizome of *Ligusticum chuanxiong* Hort. (Umbelliferae), is widely prescribed for curing cardiovascular diseases for centuries [5]. Several types of components including alkaloid, phenolic acid and phthalides have been isolated and identified during the past decades [6,7]. Among them, tetramethylpyrazine (TMP), ferulic acid and various phthalides were reported to be the bioactive components [8–10]. Up to now, studies of Chuanxiong mainly focus on the absorption, distribution, metabolism and excretion of a few isolated bioactive compounds, such as TMP, ferulic acid, ligustilide, senkyunolide A [11–18]. They can be absorbed into plasma after administration of monomer compounds, distributed to tissues, then metabolized and excreted from the organism. In this process, several common metabolic reactions occurred, including dehydrogenation, oxidation, hydroxylation, conjugation with glucuronic acid, sulphuric acid, glutathione and cysteine [12–18]. However, one or a few bioactive components used for *in vivo* studies are not sufficient to represent and reflect the overall efficacy of Chuanxiong. It was reported that ferulic acid exhibited distinctly different absorption after oral administration of pure ferulic acid and Chuanxiong extract at the equal dose [19]. Similarly, the clearance and metabolism of ligustilide after oral administration of Chuanxiong extract was significantly different from that dosed in its pure form [20]. These studies suggest that components present in the extract could influence the pharmacokinetics of certain bioactive monomer. Therefore, it is essential to establish a systemic method to real the potential bioactive components of Chuanxiong and their metabolites, which was scarcely investigated at present. Only Liu et al. analyzed the fingerprint chromatograms of chemical compositions in body fluid of rats [21]. It revealed that 10 components including nine prototypes and one metabolite were absorbed into blood. The most absorbed composition was appeared

* Corresponding author. Fax: +86 411 84379756.
E-mail address: hbxiao@dicp.ac.cn (H. Xiao).

0731-7085/$ – see front matter © 2011 Elsevier B.V. All rights reserved.
doi:10.1016/j.jpba.2011.08.010

at 60 min after oral administration. However, since the bioactive components, often interfered by endogenous metabolites and proteins, are diverse and their concentrations are quiet low, it is hard to identify them and their metabolites and subsequently to construct the metabolic pathways of them.

In the present study, serum pharmacochemistry was adopted to reveal bioactive components of Chuanxiong and their metabolites. The *in vivo* fingerprint chromatogram was obtained and further compared with that of RCD. As a result, 25 compounds including 13 absorbed components and 12 conjugated metabolites were detected simultaneously and identified by on-line structure elucidation. Then the *in vivo* metabolic pathways of chemical constituents of Chuanxiong in rat plasma were exploringly proposed. This investigation would effectively narrow the range of potentially bioactive constituents of Chuanxiong and shed light to its action mechanism.

2. Experimental

2.1. Chemicals and reagents

HPLC-grade acetonitrile was purchased from Fisher Chemicals (Fisher Chemicals, USA). HPLC-grade methanol, analytical-grade ethyl acetate and acetic acid were obtained from Yuwang (Yuwang, China). Water was purified with a Milli-Q system (Millipore, Bedford, USA). Senkyunolide I, senkyunolide A, ligustilide and levistolide A were purified from *Rhizoma Chuanxiong* in our laboratory and their structures were confirmed by comparison of their UV, MS data with the literature [22]. The purity of each isolated compound was determined to be above 95% by HPLC analysis. TMP and ferulic acid were purchased from the National Institute for the Control of Pharmaceutical and Biological Products (Beijing, China). The *Rhizoma Chuanxiong* was purchased from local herb stores in Provinces of Sichuan (Sichuan, China). The crude drug of high quality was authenticated by prof. Jinhai Yi (Sichuan Academy of Chinese Medicine Sciences).

2.2. Instrument and conditions

HPLC–UV analysis was carried out on a Waters Alliance 2690 chromatographic system (Waters Corp., Milford, USA) equipped with auto sampler, vacuum degasser and diode-array detector. Chromatographic separation was carried out on an Inertsil ODS-3 column (4.6 mm × 250 mm, 5 μm) and the temperature of column oven was maintained at 35 °C. The mobile phase consisted of acetonitrile (A), and 0.1% acetic acid (B). A gradient program was adopted as follows: 5–10% A from 0–5 min, 10–70% A from 5 to 45 min, 75–100% A from 45 to 60 min. UV spectra were recorded from 210 nm to 400 nm and the detection wavelength was set at 280 nm. The flow rate was set at 1.0 mL/min and split with a post-column stream splitter with a ratio of 1/4 to mass spectrometer.

MS experiments were performed on a TSQ triple-quadrupole mass spectrometer (Thermo, San Jose, CA, USA) equipped with an ESI interface. The ionization parameters were set as follows: spray voltage 4.0 kV; heated capillary temperature 325 °C; sheath gas at 40 psi and auxiliary gas at 20 AU. Agron at 3 torr was used as collision gas for the collision induced dissociation (CID). The mass spectrometry was programmed to perform full scan analysis over mass range of m/z 100–1000 in alternating positive and negative ionization mode. The collision energy of dissociation was set at 25 eV for ligustilide, while 20 eV for the other components in the MS/MS.

2.3. Preparation of Rhizoma Chuanxiong decoction (RCD)

240 g dry powder of Chuanxiong was immersed in 1.8 L of 70% ethanol overnight. The mixture was extracted by reflux extraction for 2 h at 80 °C. After filtered, the residue was further extracted with 1.6 L of 70% ethanol for 1 h. The filtered supernatants were combined and evaporated to dryness under reduced pressure at 60 °C. The dried residue was dissolved in water to obtain an oral solution of RCD with a concentration of 2 g herb per decoction.

2.4. In vivo study

Eight Sprague-Dawley rats (200–300 g body weight) were purchased from the laboratory animal center of Sichuan Academy of Chinese Medicine Sciences (Sichuan, China) and divided into two groups (group A, drug group for dosed rat plasma, $n = 5$; group B, control group for blank rat plasma, $n = 3$) and kept in a breeding room. The animals were fasted for 12 h with free access to water before the experience. RCD was administered orally to the rats of group A at a dose of 10 mL RCD/kg body weight. Equal dose of distilled water was orally administered to the rats of group B. The rats were continuously administered twice a day. Sixty minutes after the fifth drug administration, the animals were sacrificed by decapitation. The blood samples were collected and centrifuged at 3000 rpm for 10 min to obtain plasma samples, which were freeze-dried immediately, stored at −70 °C until analysis. All procedures were in accordance with the National Institute of Health's guidelines in principles of animal care.

2.5. Sample preparation

0.25 g plasma samples were added into a 10 mL polypropylene test tube and extracted with 4 mL methanol–ethyl acetate (1:1, v/v) for three times, by which the objective components were extracted and the protein was precipitated. Extraction was performed by vortexing for 20 s, ultrasonicating for 10 min and centrifuging at 12,000 rpm for 5 min. The supernatants were combined and evaporated to dryness under a stream of nitrogen at 40 °C. Then the dried residue was dissolved in 0.5 mL methanol–water (1:1, v/v) and centrifuged at 12,000 rpm for 10 min. An aliquot of 40 μL supernatant was injected into HPLC–MS system for analysis.

3. Results and discussion

3.1. Optimization of HPLC–MS conditions

Alkaloid, phenolic acid and phthalides are often considered as the main constituents of Chuanxiong. TMP and ferulic acid as the representatives of alkaloid and phenolic acid were purchased, while senyunolide I, ligustilide and levistolide A, as main constituents of hydroxylated phthalides, alkyl phthalides and dimeric phthalides, respectively, were purified from Chuanxiong in our laboratory. These reference compounds were used for optimizing the HPLC–MS conditions.

To separate and determine all constituents in a single analysis, a long gradient elution method was developed and acetonitrile–water rather than methanol–water was chosen as mobile phase, owing to the former had high elution efficiency and less interference in MS. However, possibly due to ionization of acidic and hydroxyl groups, the peak of ferulic acid was not observed or tailed obviously. Thus 0.1% acetic acid rather than water was selected as the mobile phase, which usually has the function of enhancing the intensity of positive ion.

UV spectra of reference compounds were obtained by using the diode array detector in the range of 210–400 nm. TMP shows

Table 1
HPLC–UV–ESI-MS identification of the constituents in *Rhizoma Chuanxiong* decoction (RCD).

No.	T_R	Positive ion	Negative ion	UV (λ_{max})	MW	Identification
1	16.35		135 (100)	209, 295	136	Tetramethylpyrazine
2	20.92	195(10), 177(100)	193 (100)	234, 294, 320	194	Ferulic aicd
3	21.39	250(100), 227(60), 209(35), 191(25)		292	226	Senkyunolide N
4	22.55	250(100), 227(50), 209(35), 191(20)		278	226	Senkyunolide J
5	23.82		367(100), 191(40)	282, 323	368	Feruloylquinic acid
6	23.86	248(100), 207(30)		276	224	Senkyunolide I
7	24.73	248(100), 207(25)		276	224	Senkyunolide H
8	25.02	223(100), 205(30)		282	222	4,7-Dihydroxy-3-butylphthalide
9	26.22		515(30), 353(100), 181(20), 178(5)	245, 294, 327	516	Dicaffeoylquinic acid
10	28.03		515(20), 353(100)	248, 294, 327	516	Dicaffeoylquinic acid
11	30.50		515(50), 353(100)	292, 317	516	Dicaffeoylquinic acid
12	31.63	223(100), 205(50)	221(100), 177(60)	285	222	Senkyunolide D
13	31.95		515(100), 353(55)	292, 317	516	Dicaffeoylquinic acid
14	33.81	232(35), 209(10), 191(100)	207(90), 163(100)	283	208	Senkyunolide G
15	34.31	207(15), 189(100)	205(100), 161(90)	237, 266, 346	206	Senkyunolide F
16	35.26	248(100), 207(33), 189(35)	205(100), 161(35)	291	206	3-Butyl-4-hydroxyphthalide
17	36.20	248(90), 207(100), 190(35)	205 (100)	292	206	Isomer of 3-butyl-4-hydroxyphthalide
18	36.78	320(15), 279(100)		273	278	Senkyunolide M
19	37.15	246(100), 205(45)	203 (100)	225, 253	204	Senkyunolide B or C
20	38.09	320 (15), 278.8(100)	277 (100)	273	278	Senkyunolide Q
21	38.13	246(55), 205(100)	203 (100)	225, 264, 331	204	Senkyunolide E
22	38.85	246(100), 205(30)	203 (100)	220, 265, 328	204	(E)-senkyunolide E
23	40.12	234(100), 193(30), 175(15),		278	192	Senkyunolide A
24	40.99	232(100), 191(25), 173(40), 145(40)		273	190	Butylphthalide
25	41.86	189 (100)			188	E-butylidenephthalide
26	42.66	236(80), 195(15), 177(25), 149(100)		267, 326	194	Cnidilide
27	42.95	232(100), 191(35), 173(10), 145(25)		288, 319	190	E-ligustilide
28	43.75	236(100),195(60), 177(35), 149(55)		260	194	Neocnidilide
29	44.55	232(100),191(35),173(10),		281, 325	190	Z-ligustilide
30	45.05	189(100), 171(50)		234, 259, 312	188	Butylidenephthalide
31	47.01	399(75), 381(50), 232(100), 191(80)		281	380	Dimer
32	49.19	398(20),381(20), 232(100), 191(30)		281	380	Dimer
33	50.20	383(100), 424(25), 234(30)		273	382	Dimer
34	50.78	405(15), 383(100)		275	382	Dimer
35	51.58	424(25), 383(1000		220, 282	382	Dimer
36	52.60	444(100), 403(25), 381(35), 232(50)		220, 282	380	Levistolide A
37	53.47	446(100), 405(40), 383(90)		227, 276	382	Dimer
38	54.55	381(20), 232(100), 191(45)		294	380	Dimer
39	55.35	444(80), 381(100), 232(35)		271	380	Dimer
40	55.86	444(75), 403(30), 381(100)		276	380	Dimer

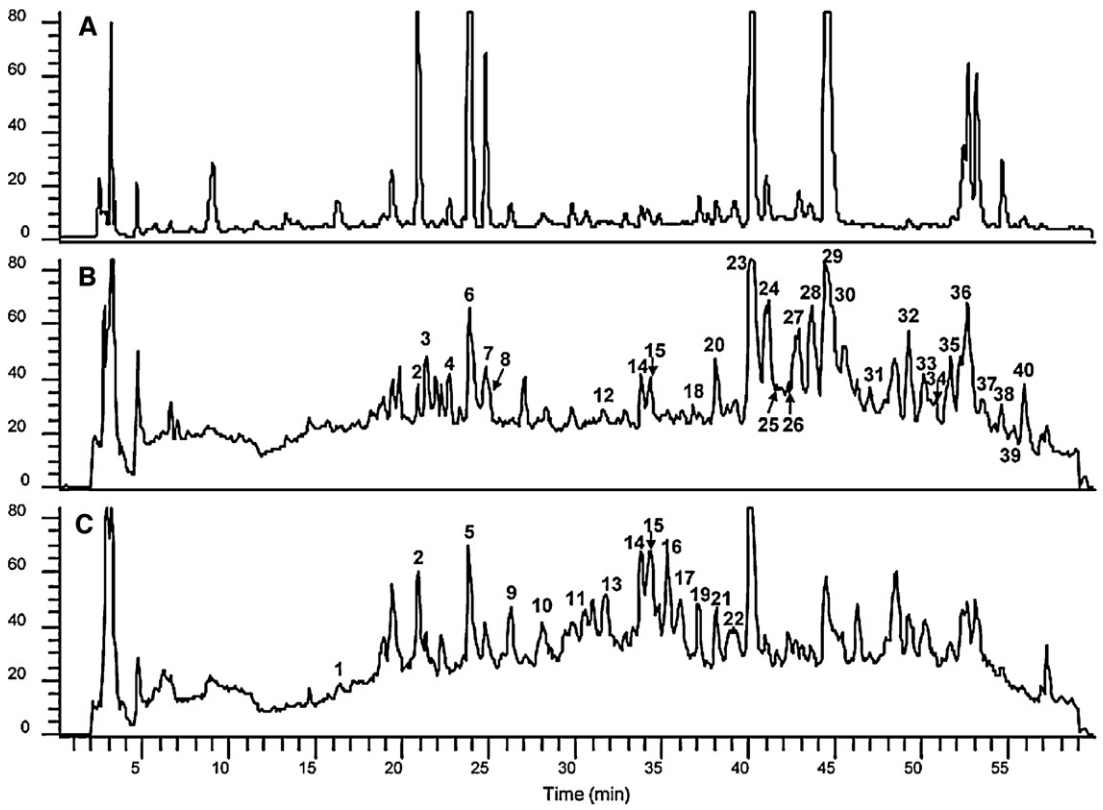

Fig. 1. Chromatograms of *Rhizoma Chuanxiong* decoction by HPLC–UV–MS. (A) UV chromatogram at 280 nm. (B) TIC chromatogram in positive ESI mode. (C) TIC chromatogram in negative ESI mode.

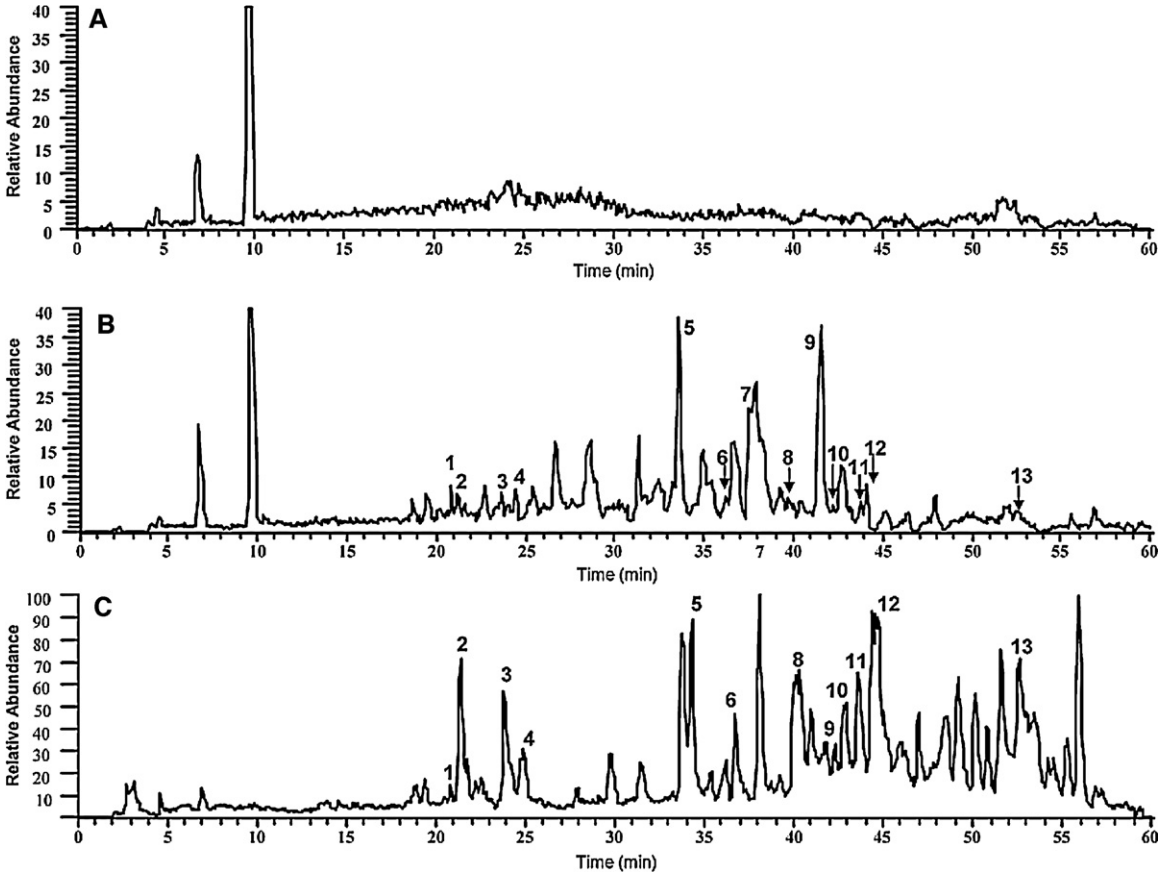

Fig. 2. Extracted ion chromatograms of 13 absorbed compounds in positive ion mode: (A) blank rat plasma, (B) dosed rat plasma collected at 60 min after oral administration of RCD and (C) *Rhizoma Chuanxiong* decoction.

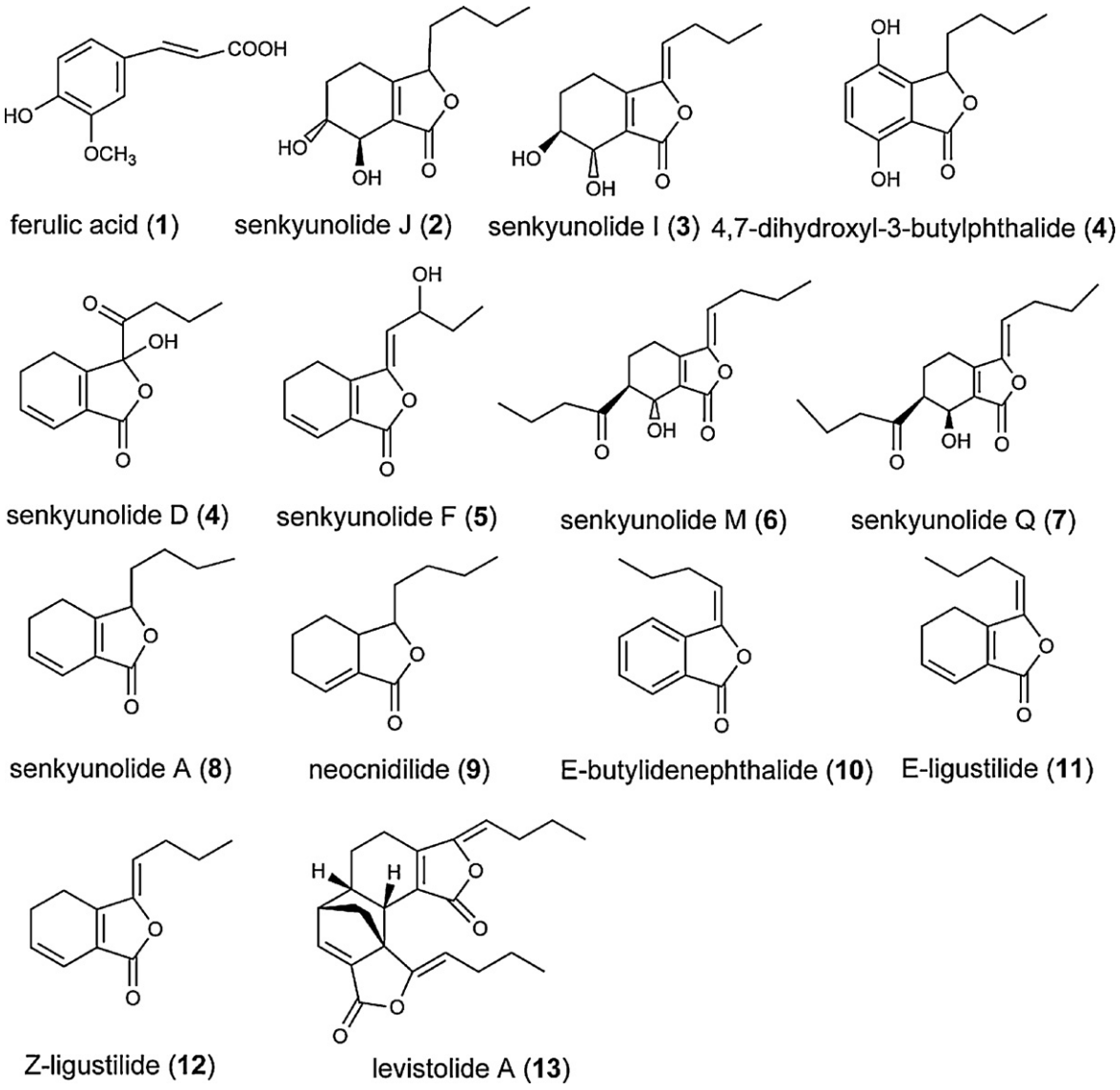

Fig. 3. Chemical structures of 13 absorbed compounds in prototype identified in the dosed rat plasma.

maximum absorption at 209 and 295 nm. Ferulic acid has maximum absorption at 234, 320 nm and a shoulder peak at 294 nm. Senkyunolide I, senkyunolide A and levistolide A all have maximum absorption at approximately 276 nm, while ligustilide at 281, 325 nm. Therefore, 280 nm was chosen for simultaneous determination of all target compounds.

In the case of MS detection, the ionization parameters were tentatively optimized and chosen as mentioned in Section 2.2. Under the conditions, ferulic acid exhibited strong $[M-H]^-$ ion in negative ion mode and weak $[M+H]^+$ ion in positive ion mode, whereas phthalides showed abundant $[M+H]^+$ ion, adduct ions $[M+H+CH_3CN]^+$or $[M+Na+CH_3CN]^+$ and a fragment ion $[M+H-H_2O]^+$ in positive ion mode. Therefore the analysis was carried out in alternating positive and negative ion mode. Furthermore, for propose of obtaining the most abundant MS/MS information, the collision energy of dissociation was also optimized. As a result, it was set at 25 eV for ligustilide, while 20 eV for the other components. Based on the optimized conditions, the limit of detection of ferulic acid, senkyunolide I, senkunolide A, ligustilide and levistolide A were determined to be 12.6 ng/mL, 28.5 ng/mL, 10.1 ng/mL, 17.0 ng/mL and 16.9 ng/mL, respectively.

3.2. Characteristic UV spectra and MS patterns of alkaloid, phenolic acid and phthalides from Chuanxiong

Different kinds of reference compounds mentioned above were used for exploring the UV features and fragmentation patterns by HPLC–ESI-MS/MS.

Tetramethylpyrazine as a main alkaloid, with maximum absorption at 209 and 295 nm, is inclined to obtain a hydrogen ion in MS, resulting in a dominate protonated molecular ion $[M+H]^+$ at m/z 137 in positive ion mode. Due to the relative stability of hetero aromatic ring, the main fragment ion at m/z 122 was generated by removal of CH_3 in side chains from the $[M+H]^+$ ion.

Ferulic acid showed maximum absorption at 234, 320 nm and a shoulder peak at 294 nm, the typical UV spectra of phenolic acid, based on which these type of compounds are preliminary assigned to. Due to the existence of hydroxyl group, it exhibited strong $[M-H]^-$ at m/z 193 and relative weak $[M+H]^+$ at m/z 195, indicating the MW of 194. The negative prominent fragment ions at m/z 179, 149 and 135 were generated by losses of CH_2, CO_2 and both of them from $[M-H]^-$ ion, corresponding to the methoxyl group and carboxyl group on the side chains of aromatic ring.

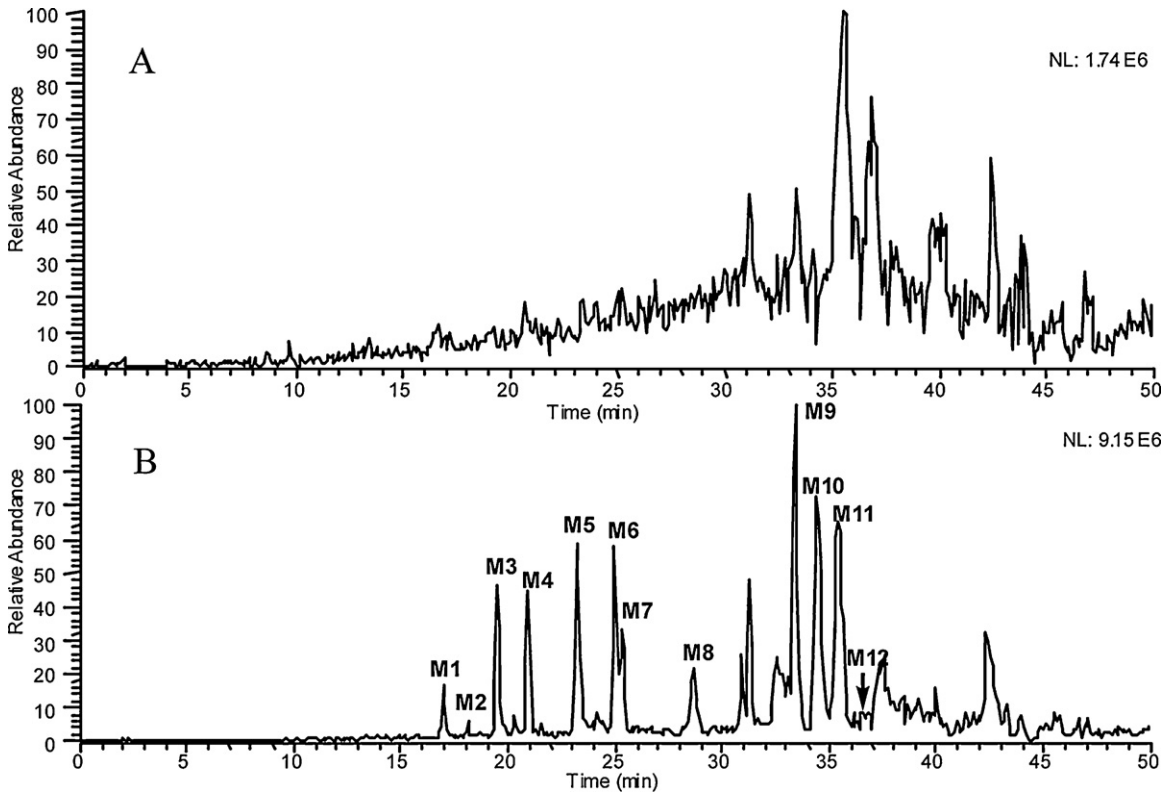

Fig. 4. Extracted ion chromatograms of 12 conjugated metabolites: (A) blank rat plasma, (B) dosed rat plasma collected at 60 min after oral administration of RCD.

Ligustilide showed abundant protonated molecular ion $[M+H]^+$ and adduct ion $[M+H+CH_3CN]^+$ in positive ion mode, based on which the MWs of alkyl phthalides can be determined. In the MS/MS spectra, characteristic fragment ions at *m*/*z* 173, 145 were abundantly generated by loss of H_2O and successive loss of CO through ring-opening, corresponding to α, β-unsaturated lactone, the common group of phthalides. The other ions were further produced by losses of different alkyl groups from the 145 through ring arrangement.

Compared with alkyl phthalides, hydroxylated phthalides usually possess one or two hydroxyl groups in their structures. Senkyunolide I with two hydroxyl groups not only showed weak $[M+H]^+$ at *m*/*z* 225, but more higher intensity ion $[M+H-H_2O]^+$ 207 and its adduct ion $[M+H-H_2O+CH_3CN]^+$ 248 in positive ion mode, indicating the MW of 224. The dominant fragment ions at *m*/*z* 207, 189 were produced by loss of one and two waters from $[M+H]^+$ ion, corresponding to the two hydroxyl groups. Similar to alkyl phthalides, the other ions at *m*/*z* 171, 161, 147 were further produced by loss of H_2O, CO, C_3H_6 from 189, corresponding to α, β-unsaturated lactone and double bond at position C3–C10. In other words, besides the ions produced by losses of one or two water, the other fragment ions of hydroxylated phthalides were usually generated in the similar ways as the corresponding alkyl phthalides did.

Levistolide A, polymerized by two molecular ligustilide, has the MW of 380. That is further confirmed by $[M+H]^+$ ion, its adduct ions $[M+Na]^+$ and $[M+Na+CH_3CN]^+$ in positive ion mode. The CID spectrum of $[M+H]^+$ produced a dominate fragment ion $[M+H-C_{12}H_{14}O_2]^+$ at *m*/*z* 191 by loss of one molecular ligustilide, which is also the $[M+H]^+$ ion of ligustilide. Then ligustilide produced the other ions as described previously.

3.3. Identification of constituents in RCD

A total of 40 peaks including 1 alkaloid, 6 phenolic acids, 8 alkyl phthalides, 15 hydroxylated phthalides, along with 10 dimeric phthalides were separated and identified by HPLC–ESI-MS in alternating positive and negative ion mode (see Fig. 1). Based on the obtained UV features, MS, MS/MS spectra, peaks 1, 2, 6, 23, 29, 36 were tentatively identified as TMP, ferulic acid, senkyunolide I, senkyunolide A, ligustilide, levistolide A, respectively. Further compared these UV and MS data with those of corresponding reference compounds, mentioned in the above section, they were unequivocally confirmed. It demonstrates that the established HPLC–MS is suitable for identifying these compounds and can be used in this study. According to the characteristics summarized above, the other peaks were identified by their UV features and MS data, which are showed in the following. The identified components are listed in Table 1.

Phenolic acid except for ferulic acid were polymerized by one or two ferulic acid or caffeic acid with quinic acid. Based on the typical UV spectra, peaks **5** and **9**–**13** were preliminary assigned to phenolic acid. Besides strong $[M-H]^-$ ion, the typical and major fragment ions were generated by losses of feruoyl [ferulic acid–H_2O] or caffeoyl [caffeic acid–H_2O] from $[M-H]^-$ ion depending on their structures. For peak **5**, the major fragment ion at *m*/*z* 191 was produced by loss of the group of feruoyl, corresponding to the $[M+H]^+$ ion of quinic acid. Thus it was identified as feruloylquinic acid. Peaks **9**–**13** exhibited strong fragment ion at *m*/*z* 353 by loss of the group of caffeoyl from $[M+H]^+$ ion at *m*/*z* 515. Thus, they were considered as the isomers of dicaffeoylquinic acid [23].

Peaks **24**–**28** and **30** were tentatively assigned to be alkyl phthalides by intense protonated molecular ion $[M+H]^+$, solvent adduct ion $[M+H+CH_3CN]^+$ and characteristic fragment ions

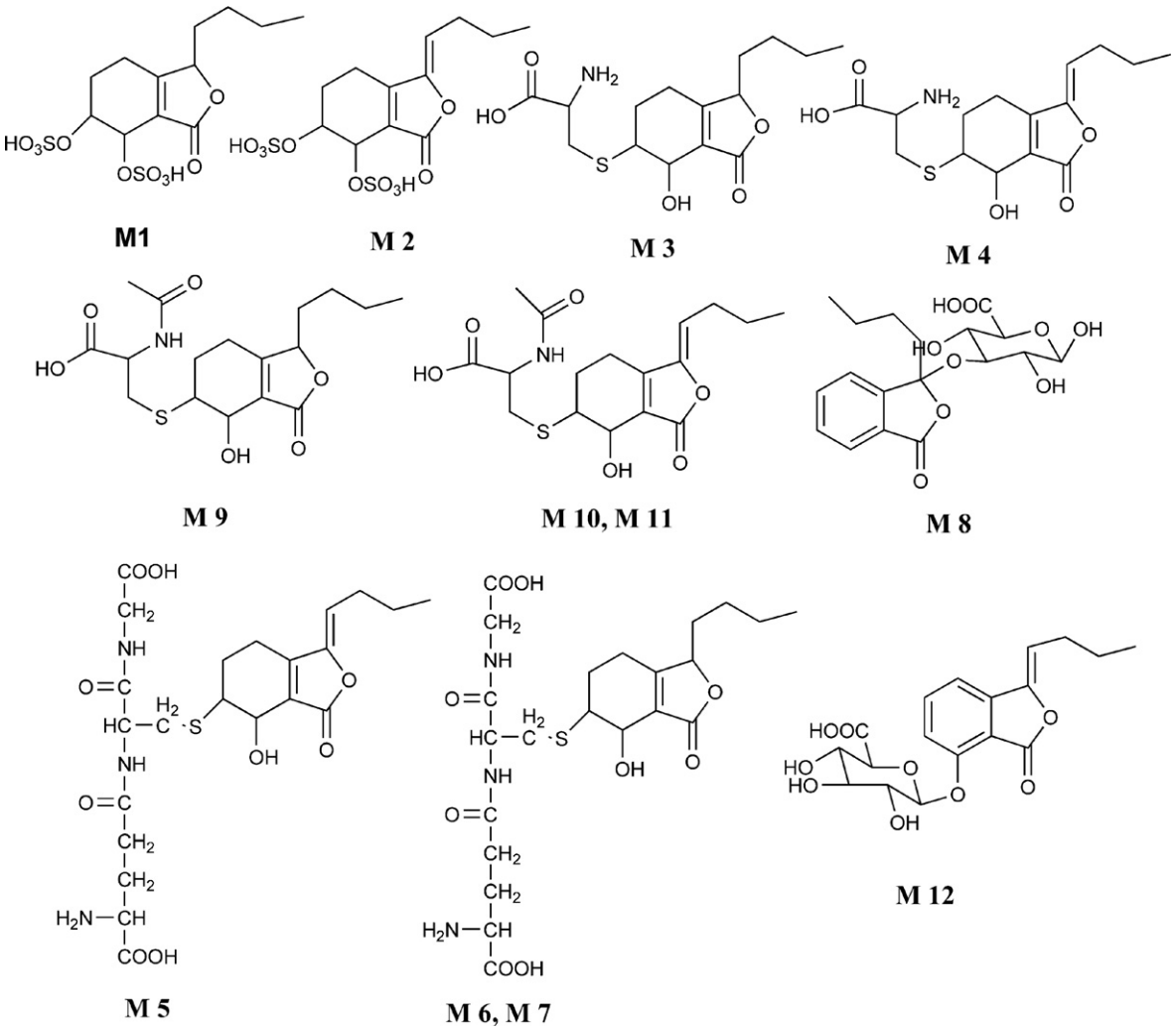

Fig. 5. Chemical structures of 12 conjugated metabolites in the dosed rat plasma.

$[M+H-H_2O]^+$, $[M+H-H_2O-CO]^+$, $[M+H-C_3H_6]^+$ or $[M+H-C_4H_8]^+$. Peaks **24**, **27**, **29** were isomers of butylphthalide/E-ligustilide/Z-ligustilide by referring to the literature [24]. For these isomers, they can be distinguished by their different UV spectra and retention behaviors. The UV spectra of **24** showed maximum absorption at 280 nm, which was different from that of **27** and **29**, i.e., the maximum absorption at 280 and 325 nm. Thus **24** was identified as butylphthalide, while **27** and **29** identified as a pair of ligustilide. In the reverse phase chromatography elution procedure, Z-form phthalides are eluted out later than the corresponding E-form. From this point, **29** were identified as Z-ligustilide while 27 as E-ligustilide. In this way, the isomers of **26** and **28**, **25** and **30** were also distinguished and shown in Table 1.

Isomers of **3**, **4** and **8**, **12**, similar to **6**, **7**, incline to losses of one and two molecular water from the $[M+H]^+$ ion, resulting in the dominate fragment ions $[M+H-H_2O]^+$ and $[M+H-2H_2O]^+$. Thus they are considered as the hydroxylated phthalides with two hydroxyl groups in their structures. Peaks **14**–**17**, **19**, **21**, **22** showed not only the $[M+H]^+$ ion, intense ion $[M+H-H_2O]^+$ and its adduct ion $[M+H-H_2O+CH_3CN]^+$ in positive ion mode, but also dominate ion $[M-H]^-$ in negative ion mode, indicating that they were hydroxylated phthalides with one hydroxyl group. Similarly, peaks **18** and **20**, with MW of 278, were considered as derivatives of senkyunolide I by substituting the hydroxyl group with oxyproxyl group at C6 position [25]. Similar to isomers of alkyl phthalides, these isomers were also distinguished by their UV spectra and retention behaviors, except for peaks **7**, **12** and **16**, **17**. The results of identification are shown in Table 1.

Similar to the MS spectra of levistolide A, peaks **31**, **32**, **36** and **38**–**40** with MW of 380 were tentatively assigned to isomers of dimeric phthalides polymerized by two molecular ligustilide. Compared with levistolide A. The MWs of peaks **33**–**35** and 3**7** can be clearly determined to 382. They showed two main fragment ions $[M+H-C_{12}H_{16}O_2]^+$ at *m/z* 191 and $[M+H-C_{12}H_{14}O_2]^+$ at *m/z* 193 by loss of senkyunolide A and ligustilide, respectively. Thus they were identified as dimeric phthalides polymerized by ligustilide and senkyunolide A. But due to lack of reference compounds, these isomers are failed to be differentiated since they possess the same MS spectra [26].

3.4. Detection of the components absorbed into rat plasma in prototype

Dosed rat plasma samples obtained at 60 min after oral administration of RCD and blank rat plasma samples were analyzed under the established HPLC–MS conditions. By examining total ion current chromatograms (TICs), the absorbed components and metabolites failed to be discovered due to their low concentrations. In order to improve the detection sensitivity, the extracted ion chromatograms (EICs) were adopted. First of all, protonated molecular ions of the identified components in RCD were used one by one to obtain EICs from dosed rat plasma, blank rat

Table 2
HPLC/MS^n data and identification of metabolites in rat plasma.

No.	T_R	Metabolic reaction	Shifts of exact mass	MS (pos.) (m/z)	MS/MS (pos.) (m/z)	Identification
M1	16.94	Sulfation with senkyunolide J	226 + 2 × 80	$[M+Na]^+$, 409 $[M+H]^+$, 387	284, 209, 191, 163	Disulphate conjugate of senkyunolide J
M2	18.08	Sulfation with senkyunolide I	224 + 2 × 80	$[M+Na]^+$, 407 $[M+H]^+$, 385	282, 207, 189, 162	Disulphate conjugate of senkyunolide I
M3	19.48	Senkyunolide J conjugated wtih cysteine	226 + 103	$[M+Na]^+$, 352 $[M+H]^+$, 330 $[M+H-COOH]^+$, 284	284, 209, 191, 163,153,	Cysteine conjugate of senkyunolide J
M4	20.89	Senkyunolide I conjugated wtih cysteine	224 + 103	$[M+Na]^+$, 350 $[M+H]^+$, 328 $[M+H-COOH]^+$, 282	282, 207, 189, 179, 165	Cysteine conjugate of senkyunolide I
M5	23.17	Senkyunolide J conjugated with glutathione	226 + 289	$[M+Na]^+$, 538 $[M+H]^+$, 516 $[M+H-75]^+$, 441 $[M+H-129]^+$, 387	441, 387, 369, 284, 191	Glutathione conjugate of senkyunolide J
M6	24.92	Senkyunolide I conjugated with glutathione	224 + 289	$[M+H]^+$, 514 $[M+H-75]^+$, 439 $[M+H-129]^+$, 385	439, 385, 282, 207, 179	Glutathione conjugate of senkyunolide I
M7	25.27	Senkyunolide I conjugated with glutathione	224 + 289	$[M+H]^+$, 514 $[M+H-75]^+$, 439 $[M+H-129]^+$, 385	439, 385, 282, 207, 179	Glutathione conjugate of senkyunolide I
M8	28.61	Gluronidation with 3-hydroxybutylphthalide	188 + 18 + 176	$[M+H]^+$, 383	207, 191, 158	3-Hydroxybutylphthalide-3-O-β-D-glucuronide
M9	33.41	Senkyunolide J conjugated wtih acetycysteine	226 + 145	$[M+H]^+$, 372 $[M+H-O]^+$, 356	329, 284, 209, 191,	Acetylcysteine conjugate of senkyunolide J
M10	34.40	Senkyunolide I conjugated wtih acetycysteine	224 + 145	$[M+Na]^+$ 392 $[M+H]^+$, 370	327, 282, 207, 189	Acetylcysteine conjugate of senkyunolide I
M11	35.36	Senkyunolide I conjugated wtih acetycysteine	224 + 145	$[M+Na]^+$ 392 $[M+H]^+$, 370	327, 282, 207, 189,	Acetylcysteine conjugate of senkyunolide I
M12	36.59	Gluronidation with 7-hydroxybutylldenephthalide	188 + 16 + 176	$[M+H]^+$, 381	205, 187	7-Hydroxybutylidenephthalide-7-O-β-D-glucuronide.

plasma and RCD simultaneously. Secondly, by comparing these obtained EICs, peaks that were appeared both in dosed rat plasma and RCD at corresponding position but not in blank rat plasma were considered as the components absorbed into plasma in prototype. Thirdly, once these peaks were determined to be the absorbed components, the MS/MS spectra were obtained subsequently by CID. Finally by carefully comparing MS, MS/MS data, UV spectra, and retention times of these peaks obtained from dosed rat plasma with that obtained from RCD, they were further to be confirmed. According to the method described above, 13 compounds were absorbed into rat plasma in prototype and identified as ferulic acid (**1**), senkyunolide J (**2**), senkyunolide I (**3**), senkyunolide D or 4,7-dihydroxy-3-butylphthalide (**4**), senkyunolide F (**5**), senkyunolide M (**6**), senkyunolide Q (**7**), senkyunolide A (**8**), E-butylidenephthalide (**9**), E-ligustilide (**10**), neocnilide (**11**), Z-ligustilide (**12**), levistolide A (**13**). The EICs of total 13 compounds are shown in Fig. 2. Their structures are shown in Fig. 3.

From the result, it is clear that 13 absorbed compounds of total 40 compounds in RCD are the major constituents of Chuanxiong and account for about 90% of the composition, while the other minor components were not absorbed into rat plasma or their concentrations were to low to be detected. By further examining EICs of 13 compounds obtained from RCD and the dosed rat plasma, it is apparent that the pattern of absorbed components in rat plasma was significantly different from that in RCD. Alkyl phthalides presented in low concentration while hydroxylated phthalides exhibited relatively higher abundance in rat plasma in contrast with RCD. These observed changes partly originate from differences of compounds in absorption, metabolic rate or binding with plasma proteins. Another deduced factor is that alkyl phthalides could be changed into hydroxylated phthalides through some phase I reactions, such as oxidation, hydrolysis. In other words, hydroxylated phthalides, such as senkyunolide J, senkyunolide I and senkyunolide D, can be not only absorbed into plasma, but also biotransformed from alkyl phthalides through some phase I reactions.

3.5. Detection and identification of conjugated metabolites in rat plasma

The compounds absorbed into rat plasma after oral administration were further metabolized by various drug metabolizing enzymes. These metabolic reactions can be divided into two cases called phase I and phase II reactions. Phase I reactions have been already discussed in the above section. Thus phase II reactions were focused on in this section, which occurred by conjugation with endogenous molecule (glucuronic acid, amino acid, etc.) to form conjugated metabolites. These reactions can lead to structural changes and certain shifts of exact masses. For example, glucuronidation, sulfation and conjugation with L-glutamine cause 176, 80, 129 shifts of exact mass, respectively. Based on above metabolism rule of drugs [27] and MWs of the absorbed components, the MWs of probable metabolites were firstly postulated. Then EICs of the protonated molecular ion of probable metabolites were obtained from dosed rat plasma and blank rat plasma, and compared successively. New peaks discovered in dosed rat plasma samples, but not in blank rat plasma samples should be considered as the probable conjugated metabolites. Furthermore, these selected peaks were analyzed by MS/MS in product ion mode. Finally by comparing the MS, MS/MS spectra of the probable conjugated metabolites with that of corresponding original components, they were further to be confirmed. In this way, all probable conjugated metabolites were searched for and a total of 12 conjugated metabolites were tentatively identified as phthalide-related metabolites, including 6 senkyunolide I-related metabolites, 4 senkyunolide J-related metabolites and 2 butylidenephthalide-

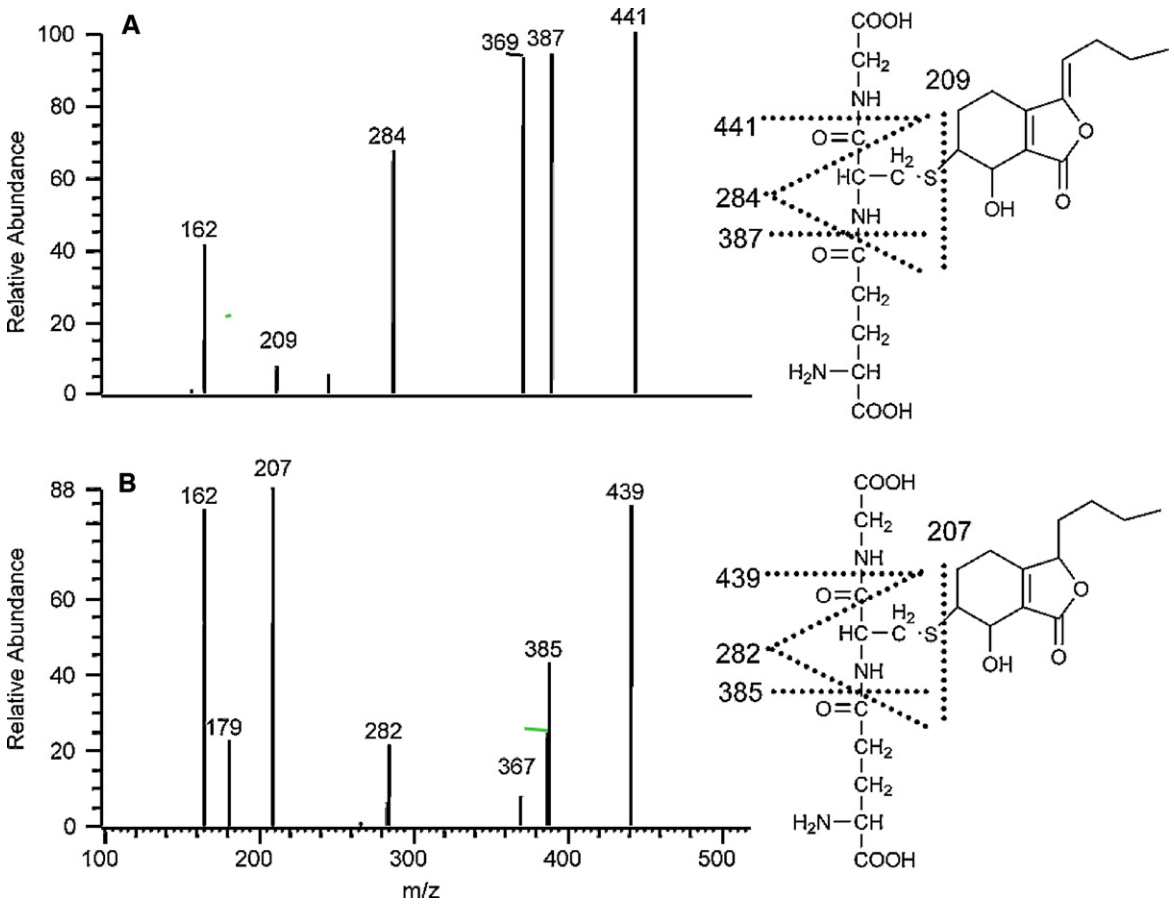

Fig. 6. ESI-MS/MS spectra of metabolites M5 (A) and M6 (B) in positive ion mode (collision energy 30 V).

related metabolites. The EICs of 12 metabolites are shown in Fig. 4. Their MS and MS/MS data are summarized in Table 2, and possible structures are presented in Fig. 5.

M2, **M4**, **M6**, **M7**, **M10**, **M11** showed similar fragment ions at *m*/*z* 207, 189, 179, 161, 165 in positive ion mode, the characteristic fragment ions of senkyunolide I. So they were tentatively assigned to be senkyunolide I-related metabolites. Similarly, **M1**, **M3**, **M5**, **M9** were identified as senkyunolide J-related metabolites owing to the presence of diagnostic fragment ions related to senkyunolide J, such as 209, 191, 163, 153. While **M8**, **M12** were designated as butylidenephthalide-related metabolites due to the shifts of exact masses, characteristic neutral losses and some diagnostic ions related to butylidenephthalide [28].

M1 exhibited $[M+H]^+$ ion at *m*/*z* 387 and $[M+Na]^+$ ion at *m*/*z* 409 in positive ion mode, indicating the MW of 386, 160 Da higher than that of senkyunolide J (226). In the MS/MS spectrum, abundant fragment ion at *m*/*z* 209, the characteristic ion of senkyunolide J, was yielded by successive losses of neutral fragment 80, 80, 18 Da, corresponding to two SO_3 units and one water unit. **M2**, with the MW of 384, produced the dominate fragment ion at *m*/*z* 207 through the similar fragment pathways. Therefore, **M1** and **M2** were identified as disulphate of senkyunolide J and senkyunolide I, respectively.

The MS spectrum of **M4** exhibited $[M+H]^+$ ion at *m*/*z* 328, adduct ion $[M+Na]^+$ at *m*/*z* 350 in positive ion mode. These characteristic ions indicated MW of 327, 103 Da higher than the MW of senkyunolide I (224), suggesting the presence of one cysteine residue in **M4**. Fragment ions at *m*/*z* 282, 207 were formed by loss of 46 Da (CH_2O_2) and 121 Da (cysteine) from the $[M+H]^+$ ion. Therefore, **M4** is designated as cysteine conjugate of senkyunolide I. Similarly, **M3** is designated as cysteine conjugate of senkyunolide J. However, by examining the structures of senkyunolide I and senkyunolide J, both C6 and C7 hydroxyl groups could conjugate with cysteine. Based on above MS data it is difficult to determine their actual reactive position. Further considering the steric hindrance, the conjugation occurred at C6 position was preferred to in this study, so as the other metabolites conjugated with one endogenous molecule from senkyunolide I or senkyunolide J.

The isomers of **M10** and **M11** showed MW of 369, 145 Da higher than that of senkyunolide I (224), 42 Da higher than that of **M3** (327), suggesting the presence of one acetycysteine residue in them. The main fragment ion at *m*/*z* 207 was produced by loss of acetycysteine (163 Da) from the protonated ion. Other fragment ions at *m*/*z* 327 and 282 were formed by removal of acetyl (43 Da) and successive loss of COOH (45 Da). Thus, **M10** and **M11** were identified as isomers of acetylcysteine conjugate of senkyunolide I. Due to the similar fragment ions $[M+H-acetyl]^+$ at *m*/*z* 329, $[M+H-acetyl-COOH]^+$ at *m*/*z* 284 and $[M+H-acetylcysteine]^+$ at *m*/*z* 209, **M9** with MW of 371 was identified as acetylcysteine conjugate of senkyunolide J.

The $[M+H]^+$ ion of **M6** and **M7** at *m*/*z* 514 showed mass shift of 289 Da (glutathione unit) from the $[M+H]^+$ ion of senkyunolide I. The fragment ions at *m*/*z* 439, 385, 282, 207 were generated by losses of glycine (75 Da), glutamic acid (129 Da), $C_5H_{12}N_2O_6$ (232 Da), GSH (307 Da) from the protonated ion, respectively. These ions are the characteristic neutral losses associated with the cleavage of GSH. Thus **M6** and **M7** were indicated as isomers of glutathione conjugate of senkyunolide I. Similarly, **M5** with protonated molecular ion at *m*/*z* 516, fragment ions at *m*/*z* 441 $[M+H-glycine]^+$, 387 $[M+H-glutamic\ acid]^+$, 284 $[M+H-GSH]^+$, was confirmed as

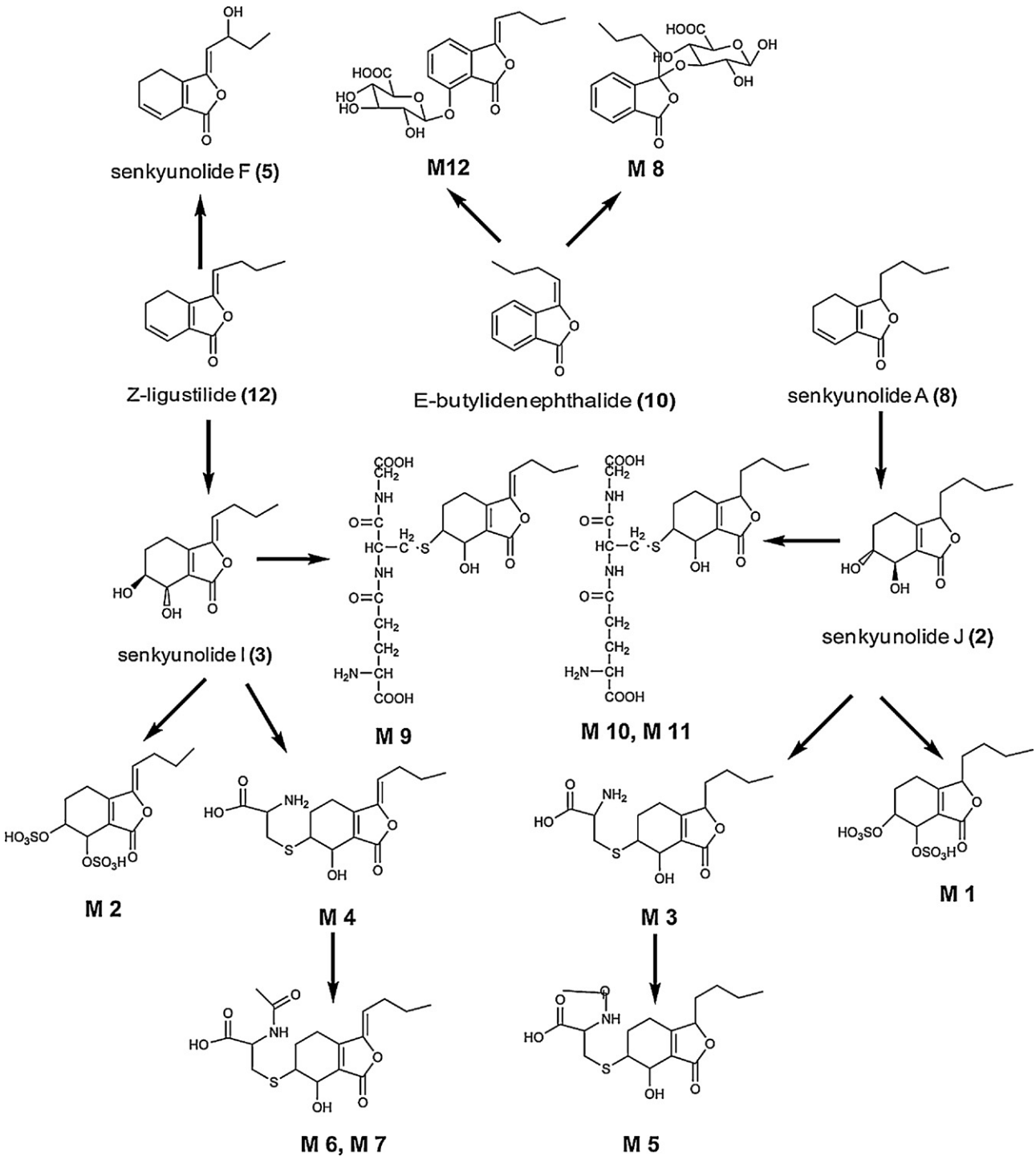

Fig. 7. The proposed *in vivo* metabolic pathways of chemical constituents in rat plasma.

glutathione conjugate of senkyunolide J. ESI-MS/MS spectra of **M5** and **M6** at positive ion mode are presented in Fig. 6.

M8, the protonated molecular ion at *m*/*z* 383, exhibited an abundant ion at *m*/*z* 207 by loss of 176 Da (glucuronide unit), the most characteristic neutral loss for glucuronide. The yielded ion at *m*/*z* 207 is 18 Da (H_2O) higher than the $[M+H]^+$ ion of butylidenephthalide, suggesting the hydrolysis of butylidenephthalide. Due to the relative stability of aromatic ring, the hydrolysis should be occurred at the C3–C10 position, through which 3-hydroxybutylphthalide was produced. Therefore, **M8** was tentatively identified as 3-hydroxybutylphthalide-3-O-β-D-glucuronide. For **M12**, a dominated ion at *m*/*z* 205 was also generated by loss of 176 Da from the protonated ion, which is 16 Da (O) higher than the protonated ion of butylidenephthalide, corresponding to hydroxylated butylidenephthalide. Thus **M12** were tentatively identified as 7-hydroxybutylidenephthalide-7-O-β-D-glucuronide.

3.6. Proposed metabolic pathways of chemical constituents in rat plasma

By examining the absorbed components and conjugated metabolites, the main *in vivo* metabolic pathways of chemical constituents in rat plasma were exploringly proposed. Besides

ferulic acid, alkyl phthalides as the main constituents of Chuanxiong were absorbed into blood after oral administration, then changed into hydroxylated phthalides under the function of some phase I reactions, including oxidation, reduction, and hydrolysis. For example, the most abundance compound ligustilide was changed into senkyunolide I and senkyunolide F, while senkyunolide A was changed into senkyunolide J. These two types of components including alkyl phthalides and hydroxylated phthalides considered as the pharmaceutical components could show their inordinate bioactive effects *in vivo*. After above progress, hydroxylated phthalides conjugated with the endogenous molecule (glucuronide acid, glutathione, amino acid, etc.) to form conjugated metabolites under the function of phase II reactions. These reactions may significantly increase their hydrophilicity, which can greatly promote excretion of the drug from organism. The proposed *in vivo* metabolic pathways of chemical constituents in rat plasma are shown in Fig. 7.

4. Conclusions

An HPLC–ESI-MS/MS method was established and applied to analysis the absorbed components and metabolites in rat plasma samples after oral administration of RCD. As a result, 13 compounds were absorbed into rat plasma in prototype and simultaneously identified by comparing their MS, MS/MS, UV spectra and retention behaviors obtained from rat plasma with that obtained from RCD. In addition, by scanning all possible metabolites in EICs mode, 12 conjugated metabolites including 6 senkyunolide I-related metabolites, 4 senkyunolide J-related metabolites and 2 butylidenephthalide-related metabolites were identified by comparing the MS, MS/MS spectra with that of corresponding original components. Furthermore the *in vivo* metabolic pathways of chemical constituents in rat plasma were predicatively proposed.

Acknowledgements

This work was financially supported by the National Natural Science Foundation of China (No. 30973873) and Key National Science and Technology Specific Projects (No. 2009ZX09502-023). Sichuan Academy of Chinese Medicine Sciences was appreciated.

References

[1] X.J. Wang, Progress and future developing of the serum pharmacochemistry of traditional Chinese medicine, China, J. Chin. Mater. Med. 31 (2006) 789–792, 835.
[2] Y.M. Hu, Y.T. Wang, S.C. Sze, K.W. Tsang, H.K. Wong, Q. Liu, L.D. Zhong, Y. Tong, Identification of the major chemical constituents and their metabolites in rat plasma and various organs after oral administration of effective Erxian Decoction (EXD) fraction by liquid chromatography–mass spectrometry, Biomed. Chromatogr. 24 (2010) 479–489.
[3] J. Peng, R.H. Liu, S.S. Dou, L. Liu, W.D. Zhang, Z.1. Chen, R.1. Xu, J.M. Ding, Analysis of the constituents in rat plasma after oral administration of Shexiang Baoxin pill by HPLC–ESI-MS/MS, Biomed. Chromatogr. 23 (2009) 1333–1343.
[4] P. Wang, Y.Z. Liang, N. Zhou, B.M. Chen, L.Z. Yi, Y. Yu, Z.B. Yi, Screening and analysis of the multiple absorbed bioactive components and metabolites of Dangguibuxue decoction by the metabolic fingerprinting technique and liquid chromatography/diode-array detection mass spectrometry, Rapid Commun. Mass Spectrom. 21 (2007) 99–106.
[5] C.J. Li, Authentication and clinical application of Chuanxiong, Strait Pharma. J. 21 (2009) 95–96.
[6] S.L. Li, S.S. Chan, G. Lin, L. Ling, R. Yan, H.S. Chung, Y.K. Tam, Simultaneous analysis of seventeen chemical ingredients of *Ligusticum chuanxiong* by on-line high performance liquid chromatography–diode array detector–mass spectrometry, Planta Med. 69 (2003) 445–451.
[7] H.X. Li, M.Y. Ding, J.Y. Yu, Separation and identification of the phthalic anhydride derivatives of *Ligusticum chuanxiong* Hort by GC–MS, TLC, HPLC–DAD, and HPLC–MS, J. Chromatogr. Sci. 40 (2002) 156–161.
[8] J. Xu, Y.K. Li, Z.J. Liang, Effects of tetramethylpyrazine and ferulic acid alone or combined on vascular smooth muscle, blood viscosity and toxicity, China, J. Chin. Mater. Med. 17 (1992) 680–682, 703–684.
[9] S.S.K. Chan, T.Y. Cheng, G. Lin, Relaxation effects of ligustilide and senkyunolide A, two main constituents of *Ligusticum chuanxiong*, in rat isolated aorta, J. Ethnopharmacol. 111 (2007) 677–680.
[10] S. Kobayashi, Y. Mimura, K. Notoya, I. Kimura, M. Kimura, Antiproliferative effects of the traditional Chinese medicine shimotsu-to, its component cnidium rhizome and derived compounds on primary cultures of mouse aorta smooth muscle cells, Jpn. J. Pharmcol. 60 (1992) 397–401.
[11] Y. Man, Y. Yu, The progress on pharmacokinetics of tetramethylpyrazine in vivo, Chin. Tradit. Herb Drugs 32 (2001) 1–2.
[12] Y.P. Ye, S.Z. Wang, J. Jiang, Studies on the metabolites of tetramethylpyrazine in human urine, Acta Acad. Med. Sin. 18 (1996) 288–291.
[13] L. Rondini, M.N. Peyrat-Maillard, A. Marsset-Baglieri, C. Berset, Sulfated ferulic acid is the main in vivo metabolite found after short-term ingestion of free ferulic acid in rats, J. Agric. Food Chem. 50 (2002) 3037–3041.
[14] R. Yan, N.L. Ko, S.L. Li, Y.K. Tam, G. Lin, Pharmacokinetics and metabolism of ligustilide, a major bioactive component in *Rhizoma Chuanxiong*, in the rat, Drug Metab. Dispos. 36 (2008) 400–408.
[15] R. Yan, G. Lin, N.L. Ko, Y.K. Tam, Low oral bioavailability and pharmacokinetics of senkyunolide A, a major bioactive component in *Rhizoma Chuanxiong*, in the rat, Ther. Drug Monit. 29 (2007) 49–56.
[16] K. Sekiya, Y. Tezuka, K. Tanaka, J.K. Prasain, T. Namba, K. Katayama, T. Koizumi, M. Maeda, T. Kondo, S. Kadota, Distribution, metabolism and excretion of butylidenephthalide of *Ligustici Chuanxiong* rhizoma in hairless mouse after dermal application, J. Ethnopharmacol. 71 (2000) 401–409.
[17] C.S. Zhao, Studied on the Pharmacokinetics of 3-*n*-Butylphthalide in Rats and Rabbits and the Transport Mechanism in Brain, Shenyang Pharmaceutical University, Shenyang, 2003.
[18] R.H. Peng, T.H. Zhou, Studied on In Vitro and In Vivo Biotranformation of Butylphthalide and its Analogues, Chinese Academy of Medical Sciences and Peking Union Medical Colleges, Beijing, 1995.
[19] X.F. Liu, X.A. Wu, Y.H. Wei, J.Y. Luo, Studies on pharmacokinetics of ferulic acid after administration of ferulic acid and *Rhizoma Chuanxiong* decoction in rat, Chin. Med. Mater. 30 (2007) 831–833.
[20] C.G. Ding, Y.X. Sheng, Y.H. Zhang, J.L. Zhang, G.H. Du, Identification and comparison of metabolites after oral administration of essential oil of *Ligusticum chuanxiong* or its major constituent ligustilide in rats, Planta Med. 74 (2008) 1684–1692.
[21] Y. Liu, R.B. Shi, B. Liu, M. Dong, Variation of chemical compositions in body fluid of rats after taking decoction of Rhiozma Chuanxiong medicinal slices orally, J. Beijing Univ. Tradit. Chin. Med. 31 (2008) 334–337.
[22] X.Z. Zhang, H.B. Xiao, Q. Xu, X.L. Li, J. Wang, X.M. Liang, Characterization of phthalides in *Ligusticum chuanxiong* by liquid chromatographic–atmospheric pressure chemical ionization–mass spectrometry, J. Chromatogr. Sci. 41 (2003) 428–433.
[23] X.Y. Yuan, M.Z. Gao, K. Wang, H.B. Xiao, C.Y. Tan, Y.G. Du, Analysis of chlorogenic acids in *Helianthus tuberosus linn* leaves using high performance liquid chromatography–mass spectrometry, Chin. J. Chromatogr. 26 (2008) 335–338.
[24] F. Yang, Y.S. Xiao, F.F. Zhang, X.Y. Xue, Q. Xu, X.M. Liang, High performance liquid chromatography–mass spectrometry analysis of Radix Angelica Sciensis, Acta Pharm. Sin. 41 (2006) 1078–1083.
[25] M. Kobayashi, H. Mitsuhashi, Studies on the constituents of umbeliferae plants XV II. Structures of three new ligustilide derivatives from *Ligusticum wallichii*, Chem. Pharm. Bull. 35 (1987) 4789–4792.
[26] S.L. Li, S.S.-k. Chan, G. Lin, L. Ling, R. Yan, H.S. Chung, Y.K. Tam, Simultaneous analysis of seventeen chemical ingredients of *Ligusticum chuanxiong* by on-line high performance liquid chromatography–diode array detector–mass spectrometry, Planta Med. 69 (2003) 445–451.
[27] M. Holčapek, L. Kolářová, M. Nobilis, High-performance liquid chromatography–tandem mass spectrometry in the identification and determination of phase I and phase II drug metabolites, Anal. Bioanal. Chem. 391 (2008) 59–78.
[28] C.Y. Li, L.W. Qi, P. Li, X.D. Wen, Y.F. Zhu, E.H. Liu, Z. Gong, X.L. Yang, M.T. Ren, Y.J. Li, X.X. Ge, Identification of metabolites of Danggui Buxue Tang in rat urine by liquid chromatography coupled with electrospray ionization time-of-flight mass spectrometry, Rapid Commun. Mass Spectrom. 23 (2009) 1977–1988.